

# Determining Reheating Temperature at Colliders with Axino or Gravitino Dark Matter

---

**Ki-Young Choi**

*Department of Physics and Astronomy, University of Sheffield,  
Sheffield S3 7RH, England, and  
Departamento de Física Teórica C-XI and Instituto de Física Teórica UAM/CSIC,  
Universidad Autónoma de Madrid, Cantoblanco, 28049 Madrid, Spain  
E-mail: K.Choi@sheffield.ac.uk*

**Leszek Roszkowski**

*Department of Physics and Astronomy, University of Sheffield,  
Sheffield S3 7RH, England, and  
Theory Division, CERN, CH-1211 Geneva 23, Switzerland  
E-mail: L.Roszkowski@sheffield.ac.uk*

**Roberto Ruiz de Austri**

*Departamento de Física Teórica C-XI and Instituto de Física Teórica UAM/CSIC,  
Universidad Autónoma de Madrid, Cantoblanco, 28049 Madrid, Spain  
E-mail: rruiz@delta.ft.uam.es*

**ABSTRACT:** After a period of inflationary expansion, the Universe reheated and reached full thermal equilibrium at the reheating temperature  $T_R$ . In this work we point out that, in the context of effective low-energy supersymmetric models, LHC measurements may allow one to determine  $T_R$  as a function of the mass of the dark matter particle assumed to be either an axino or a gravitino. An upper bound on their mass and on  $T_R$  may also be derived.

**KEYWORDS:** Supersymmetric Effective Theories, Cosmology of Theories beyond the SM, Dark Matter.

---

## Contents

<b>1. Introduction</b>	<b>1</b>
<b>2. Cosmological production of relic axino or gravitino E-WIMPs</b>	<b>4</b>
<b>3. Axino dark matter</b>	<b>8</b>
<b>4. Gravitino dark matter</b>	<b>11</b>
<b>5. Stau NLSP</b>	<b>15</b>
<b>6. Summary</b>	<b>15</b>

---

## 1. Introduction

Dark matter (DM) remains an unknown component of the Universe. While it has so far escaped detection, its existence has been convincingly inferred from gravitational effects that it imparts on visible matter through rotational curves of spiral galaxies, gravitational lensing, etc, [1]. The effects of dark matter also can be seen on large structure formation and on anisotropy of the cosmic microwave background (CMB). The CMB in particular provides a powerful tool for determining the global abundance of cold DM (CDM). Recently, the Wilkinson Microwave Anisotropy Probe (WMAP) has performed a high-accuracy measurement of several cosmological parameters. In particular, the relic density of CDM has been determined to lie in the range [2]

$$\Omega_{\text{CDM}}h^2 = 0.104 \pm 0.009. \quad (1.1)$$

Since DM has to be electrically and (preferably) color-charge neutral, from the particle physics point of view, a natural candidate for DM is some weakly interacting massive particle (WIMP). Within standard cosmology, the WIMP is produced via a usual freeze-out mechanism from an expanding plasma.

Among specific, well-motivated particle candidates for the WIMP, the by far most popular choice is a stable lightest neutralino  $\chi$  of effective low-energy supersymmetry (SUSY) models. Most efforts have gone to exploring the lightest neutralino  $\chi$  of the Minimal Supersymmetric Standard Model (MSSM) as the lightest supersymmetric particle (LSP) that, in the presence of R-parity, is stable and makes up all, or most of, the CDM in the Universe. In addition to an impressive experimental effort of direct and indirect searches for cosmic WIMPs, the Large Hadron Collider (LHC) will soon start exploring the TeV energy scale and is expected to find several superpartners and to determine their properties.

In particular, some authors have explored the feasibility of determining the neutralino's relic abundance  $\Omega_\chi h^2$  from LHC measurements [3, 4]. Their conclusion was that, under favorable circumstances, this should be possible with rather good accuracy, of order 10% or better, although this may be challenging [5]. An analogous study has also been done in the context of the Linear Collider, where accuracy of a similar determination would be much better [6].

If a WIMP signal is detected in one or more DM detection experiments, and also at the LHC a large missing-mass and missing-energy signature, characteristic of the stable neutralino, is measured and implies a similar mass, and if perhaps additionally eventually its relic abundance is determined from LHC data, even if with limited precision, and agrees with the “WMAP range” (1.1), then the DM problem will most likely be declared solved, and for a good reason.

However, such an optimistic outcome is by no means guaranteed. One realistic possibility is that the neutralino, even if it is found as an apparently stable state in LHC detectors, may not be the true LSP and therefore DM in the Universe. Instead, it could decay in the early Universe into an even lighter, and (possibly much) more weakly interacting, state, the real LSP, outside the MSSM (or some other low-energy SUSY model) spectrum. In this case, current cosmic WIMP searches will prove futile, even after improving the upper limit on the spin-independent interaction cross section on a free proton  $\sigma_p^{SI}$  from the current sensitivity of  $\sim 10^{-7}$  pb [7] down to  $\sim 10^{-10}$  pb, which is as far down as experiment can probably go given background from natural radioactivity.

Moreover, the neutralino relic abundance, as determined at the LHC, may come out convincingly outside the range (1.1). In fact, a value of  $\Omega_\chi h^2$  above about 0.1 can be easily explained in terms of a lighter LSP into which the neutralino, after its freeze-out, decayed in the early Universe [8]. This is because the relic abundance of the true LSP is in this case related to  $\Omega_\chi h^2$  by the ratio of the LSP mass  $m_{\text{LSP}}$  to  $m_\chi$ , which is less than one. If  $\Omega_\chi h^2$  comes out below (1.1), several solutions have been suggested which invoke non-standard cosmology, e.g. quintessence-driven kination [9], while preserving the neutralino as the DM in the Universe. However, if at the same time DM searches bring null results, this will provide a strong indication against the neutralino nature of DM. In contrast to the above attempts, we will consider a whole range of possible values of  $\Omega_\chi h^2$  at the LHC, both below and above 0.1. We will work instead within the framework of standard cosmology but will not assume the neutralino to be the DM in the Universe.

In this context we point an intriguing possibility of determining at the LHC the reheating temperature of the Universe. The framework we consider will therefore give us an opportunity to probe some crucial features of the early period of the Universe's history. The reheating temperature  $T_R$  is normally thought of as the temperature at which, after a period of rapid inflationary expansion, the Universe reheated (or, more properly, defrosted), and the expanding plasma reached full thermal equilibrium. Determining  $T_R$  cannot be done with the neutralino as DM since it freezes out at  $T_f \simeq m_\chi/24$ , which is normally thought to be much below  $T_R$ .<sup>1</sup> Here instead we assume a different candidate

---

<sup>1</sup>The possibility of  $T_R \lesssim T_f$  has been explored in [10] and more recently in [11]. In this case one could

for the LSP (assuming R-parity) and cold DM, whose relic density depends, at least in part, on  $T_R$ . This is the case for either an axino or a gravitino. The spin-1/2 axino (the fermionic superpartner of an axion) and the spin-3/2 gravitino (the fermionic superpartner of a graviton) are both well-motivated. The former arises in SUSY extensions of models incorporating the Peccei-Quinn solution to the strong CP problem. The latter is an inherent ingredient of the particle spectrum of supergravity models. Both, like the axion, form a subclass of extremely weakly interacting massive particles (E-WIMPs) [12]. The characteristic strength of their interactions with ordinary matter is strongly suppressed by a large mass scale, the Peccei-Quinn scale  $f_a \sim 10^{11}$  GeV in the case of axinos and the (reduced) Planck scale  $M_P \simeq 2.4 \times 10^{18}$  GeV for gravitinos. The mass of the axino  $m_{\tilde{a}}$  is strongly model-dependent and can take values ranging from keV up to TeV [13]. The mass of the gravitino  $m_{\tilde{G}}$  in gravity-mediated SUSY breaking schemes is given by  $m_{\tilde{G}} \sim M_S^2/M_P$ , where  $M_S \sim 10^{11}$  GeV is the scale of local SUSY-breaking in the hidden sector, and is expected in the GeV to TeV regime. In other schemes of SUSY breaking  $m_{\tilde{G}}$  can be (much) smaller. In this work we want to remain as model-independent as possible and will treat  $m_{\tilde{a}}$  and  $m_{\tilde{G}}$  as free parameters. Both axinos and gravitinos can be produced in decays of the neutralino (or another ordinary superpartner, e.g. the stau) after freeze-out, as mentioned above, or in thermal scatterings and decay processes of ordinary particles and sparticles in hot plasma at high enough reheating temperatures  $T_R$  - hence their relic density dependence on  $T_R$ . The possibility of axinos in a KSVZ axion framework [14] as cold DM was pointed out in [8, 15] and next studied in several papers [16, 17, 18, 19], while axinos as warm DM was considered in [20]. The gravitino as a cosmological relic was extensively studied in the literature, starting from [21, 22], more recent papers on gravitino CDM include [23, 24, 25, 26, 27, 28].

For definiteness, in this work we will first assume the lightest neutralino to be the lightest ordinary superpartner and the next-to-lightest particle (NLSP), although below we will also consider the case of the stau. Our main result is that, assuming the axino or gravitino as the true LSP and CDM, and that the (apparently stable) neutralino is discovered at the LHC and its “relic abundance”  $\Omega_\chi h^2$  is determined from LHC data, then one should be able to determine the reheating temperature in the Universe as a function of the LSP mass, or at least place an *upper bound* on it, as we show below. In the regime where thermal production dominates, in the axino case we find  $T_R \propto f_a^2/m_{\tilde{a}}$  while in the gravitino case  $T_R \propto m_{\tilde{G}}$ . Alternatively, in the non thermal production dominated regime, we find an *upper bound* on the allowed mass range of a CDM particle. Furthermore,  $\Omega_\chi h^2$  at the LHC can be expected to come out either below or above (or for that matter even accidentally agree with) the “WMAP range” (1.1).

The same holds true also in the even more striking case of the lighter stau taking the role of the NLSP instead. In this case the very discovery of an (apparently stable) charged massive particle at the LHC will immediately imply that DM is made up of some state outside the usual spectrum of low-energy superpartners. In this case, dedicated studies of the differential photon spectrum may allow one to distinguish between the axino and the

---

think of determining experimentally  $T_R$  even with the neutralino as DM.

gravitino LSP [29].

We stress that, a detection of a (seemingly) stable neutralino at the LHC will not be sufficient to prove that the neutralino is the LSP and the CDM.<sup>2</sup> Even establishing an apparent agreement of  $\Omega_\chi h^2$ , as to be determined at the LHC, with the range (1.1) will not necessarily imply the neutralino nature of DM, although admittedly it will be very persuasive. For this, a signal in DM searches must also be detected and the resulting WIMP mass must be consistent with LHC measurements of the neutralino mass.

The paper is organized as follows. In section 2, we review the thermal and non-thermal production of axinos and gravitinos and next explain our strategy for determining  $T_R$  at the LHC. In sections 3 and 4, we discuss the reheating temperature determination with axino LSP and gravitino LSP respectively, assuming the neutralino to be the NLSP. In section 5 we consider instead the lighter stau as the NLSP. We make final remarks and summarize our findings in section 6.

## 2. Cosmological production of relic axino or gravitino E-WIMPs

First we briefly review main mechanisms of producing relic axino or gravitino E-WIMPs, assumed to be the LSP, in the early Universe. Since both are neutral Majorana particles, they are produced in an analogous way. Since the interactions of axino and gravitino are strongly suppressed with respect to the Standard Model interaction strengths by  $f_a$  and  $M_P$ , respectively, they can be in thermal equilibrium only at very high temperatures of order  $10^{11}$  GeV. Axinos and/or gravitinos produced at lower temperatures are out-of-equilibrium, thus their abundance depends on the reheating temperature.

Neglecting the initial equilibrium population (which we assume to have been diluted through inflation), we consider here two generic ways to re-populate the Universe with axinos or gravitinos. One proceeds via scatterings and decay processes of ordinary particles and sparticles in thermal bath. Its efficiency is proportional to their density in the plasma which is a function of  $T_R$ . Following [15] we call it *thermal production* (TP). The other, dubbed *non-thermal production* (NTP) refers to (out-of-equilibrium) decays of the NLSPs, after their freeze-out, to E-WIMPs. In addition, there could be other possible mechanisms contributing to E-WIMP population, e.g. through inflaton decay, but they are much more model dependent and will not be considered here.

**Thermal production at high  $T_R$ .** In considering thermal production of E-WIMPs we compute their yield  $Y_{\text{LSP}}^{\text{TP}} \equiv n_{\text{LSP}}/s$ , where  $n_{\text{LSP}}$  is their number density and  $s$  is the entropy density. To this end, we integrate the Boltzmann equation up to the reheating temperature  $T_R$ . Their thermal abundance is then given by

$$\Omega_{\text{LSP}}^{\text{TP}} h^2 = m_{\text{LSP}} Y_{\text{LSP}}^{\text{TP}} \frac{sh^2}{\rho_{\text{crit}}}, \quad (2.1)$$

---

<sup>2</sup>Note that, for the neutralino, or any other superpartner, to appear stable in an LHC detector, it is sufficient that its lifetime is longer than a microsecond or so. Of course, if it is unstable, then it will be immediately clear that the neutralino is not cosmologically relevant.

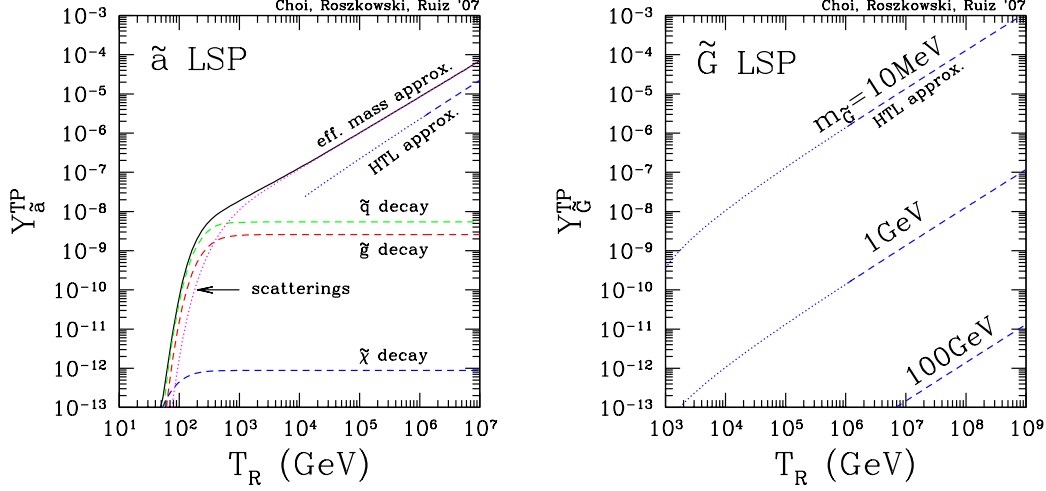


**Figure 1:** The thermal yield of axinos  $Y_{\tilde{a}}^{\text{TP}}$  (left panel) and gravitinos  $Y_{\tilde{G}}^{\text{TP}}$  (right panel) as a function of  $T_R$ . In both panels the neutralino mass is  $m_{\chi} = 300 \text{ GeV}$ , the tau mass is  $m_{\tilde{\tau}_1} = 474 \text{ GeV}$ , while gluino, squark masses are set at  $1 \text{ TeV}$ . In the left panel we take  $f_a = 10^{11} \text{ GeV}$ ; the yield scales as  $1/f_a^2$ . The black solid curve has been obtained within the effective (plasmon) mass approximation, as implemented in [15], which we use in this work. For comparison, the blue curve has been obtained in [18] by applying a hard thermal loop (HTL) technique. We also show the relative contributions to  $Y_{\tilde{a}}^{\text{TP}}$  from squark, gluino and neutralino decays. In the right panel we compute the gravitino yield following ref. [25] where the HTL technique was applied. In both panels the results obtained within the HTL formalism are more correct at  $T_R \gtrsim 10^6 \text{ GeV}$  (dashed) but less applicable at lower  $T_R$  (dotted).

where  $h$  is the dimensionless Hubble parameter and  $\rho_{\text{crit}}$  is the critical density. In other words,  $m_{\text{LSP}} Y_{\text{LSP}}^{\text{TP}} = 3.7 \times 10^{-10} (\Omega_{\text{LSP}}^{\text{TP}} h^2 / 0.1)$ , which is actually true in general.

In the case of axinos we follow the procedure described in detail in [8, 15, 16, 17]. The main production channels are the scatterings of strongly interacting (s)particles described by the dimension-five axino-gluino-gluon term

$$\mathcal{L}_{\tilde{a}} \ni i \frac{\alpha_s}{16\pi f_a} \bar{\tilde{a}} \gamma_5 [\gamma^\mu, \gamma^\nu] \tilde{g}^a F_{\mu\nu}^a. \quad (2.2)$$

The most important contributions come from 2-body processes into final states,  $i + j \rightarrow \tilde{a} + \dots$  [8, 15]. Axinos also can be produced through the decays of heavier superpartners in thermal plasma. In this work we include gluino, squark, slepton and neutralino decays. At low reheating temperatures, comparable to the mass of the decaying particle, axino production from squark decay in thermal bath gives dominant contribution [15].

In the gravitino case, the analogous dominant goldstino-gluino-gluon dimension-five term is given by [23, 25]

$$\mathcal{L}_{\tilde{G}} \ni \frac{m_{\tilde{g}}}{\sqrt{26} M_{\text{P}} m_{\tilde{G}}} \bar{\psi}_G [\gamma^\mu, \gamma^\nu] \tilde{g}^a F_{\mu\nu}^a, \quad (2.3)$$

where the goldstino  $\psi_G$  is the spin-1/2 component of the gravitino. Note the dependence on  $m_{\tilde{g}}/m_{\tilde{G}}$ , while no analogous term appears in the axino case. In computing the gravitino

yield from thermal processes we follow ref. [25]. On the other hand, we do not include gravitino production from sparticle decays in the plasma [19] which change the yield by a factor of about two.

Fig. 1 shows the yield of axinos  $Y_{\tilde{a}}^{\text{TP}}$  (left panel) and of gravitinos  $Y_{\tilde{G}}^{\text{TP}}$  (right panel) from thermal production as a function of  $T_{\text{R}}$ . Input parameters are given in the caption. As expected, in both cases the yield grows with increasing  $T_{\text{R}}$ . In the axino case, a sharp drop-off below  $T_{\text{R}} \sim 1 \text{ TeV}$  is due to Boltzmann suppression factor  $\exp(-m/T)$ , with  $m$  denoting here squark and gluino mass; at lower  $T_{\text{R}}$  superpartner decay processes become dominant but are less efficient [15].

In both axino and gravitino production from scatterings in thermal plasma, some classes of diagrams suffer from infra-red divergence. An early remedy in terms of a plasmon mass as a infra-red regulator in the gravitino case in [22] was more recently improved using hard thermal loop (HTL) technique and a finite result was obtained [24, 25]. The HTL technique is fully applicable only in cases corresponding to rather high  $T_{\text{R}} \gtrsim 10^6 \text{ GeV}$  for which, in the right panel of fig. 1, the gravitino yield is marked with a dashed line for a few representative choices of  $m_{\tilde{G}}$ . At lower  $T_{\text{R}}$  we use the same formalism but the result is less reliable (dotted parts). In the axino case an analogous calculation was performed in [18] but is of more limited use since for the axino to be CDM one requires  $T_{\text{R}} \lesssim 10^6 \text{ GeV}$  [15]. In this work in computing the axino yield we therefore follow [15] and use the plasmon mass as a regulator. The result is shown as solid line in the left panel of fig. 1 and labelled “effective mass approximation”. For comparison, the blue line shows the result obtained in [18] using the HTL technique which is more correct than our treatment in the regime marked by a dashed line but less reliable in the one marked by a dotted one ( $T_{\text{R}} \lesssim 10^6 \text{ GeV}$ ). In any case, the difference is of order a few which is not important for our purpose.

Since the axino yield from thermal production  $Y_{\tilde{a}}^{\text{TP}}$  is basically independent of the axino mass, until it becomes comparable to the masses of MSSM sparticles, its relic abundance  $\Omega_{\tilde{a}}^{\text{TP}} h^2$  is proportional to  $m_{\tilde{a}}$  and can then be expressed as [15]

$$\Omega_{\tilde{a}}^{\text{TP}} h^2 = 0.1 \left( \frac{m_{\tilde{a}}}{100 \text{ GeV}} \right) \left( \frac{Y_{\tilde{a}}^{\text{TP}}}{3.7 \times 10^{-12}} \right). \quad (2.4)$$

At high enough  $T_{\text{R}}$  thermal production is dominated by scattering processes and an application of the HTL leads to the following formula [18]

$$\Omega_{\tilde{a}}^{\text{TP}} h^2 \simeq 5.5 g_s^6 \ln \left( \frac{1.108}{g_s} \right) \left( \frac{m_{\tilde{a}}}{0.1 \text{ GeV}} \right) \left( \frac{10^{11} \text{ GeV}}{f_a} \right)^2 \left( \frac{T_{\text{R}}}{10^4 \text{ GeV}} \right), \quad (2.5)$$

where  $g_s$  is temperature-dependent strong coupling constant, which in the above expression is evaluated at  $T_{\text{R}}$ . Note that,  $Y_{\tilde{a}}^{\text{TP}} \propto T_{\text{R}}/f_a^2$ , as expected.

In the gravitino case, due to the above-mentioned gravitino mass dependence in the denominator of the dimension-five terms of the gravitino Lagrangian,  $Y_{\tilde{G}}^{\text{TP}} \propto 1/m_{\tilde{G}}^2$ , and the relic abundance calculated using a HTL technique can be expressed as [25]

$$\Omega_{\tilde{G}}^{\text{TP}} h^2 \simeq 0.27 \left( \frac{T_{\text{R}}}{10^{10} \text{ GeV}} \right) \left( \frac{100 \text{ GeV}}{m_{\tilde{G}}} \right) \left( \frac{m_{\tilde{g}}(\mu)}{1 \text{ TeV}} \right)^2, \quad (2.6)$$

where  $m_{\tilde{g}}(\mu)$  stands for the gluino mass evaluated at a scale  $\mu \simeq 1$  TeV.

**Non-thermal production from NLSP decays.** As the Universe cools down, all heavier superparticles first cascade decay into the lightest superpartners of the low-energy SUSY spectrum, in our case the NLSPs. The NLSPs then freeze out from thermal equilibrium and only later decay to LSP axinos or gravitinos. Since all the NLSPs decay into axino or gravitino LSPs, their number density is the same as that of decaying NLSP,  $Y_{\text{LSP}} = Y_{\text{NLSP}}$ , and the LSP relic abundance from non-thermal production is given by

$$\Omega_{\text{LSP}}^{\text{NTP}} h^2 = \frac{m_{\text{LSP}}}{m_{\text{NLSP}}} \Omega_{\text{NLSP}} h^2. \quad (2.7)$$

Once supersymmetric particles are found at the LHC and relevant parameters of the NLSP are determined, then its freeze-out relic abundance can be calculated by solving the Boltzmann equation (under the assumption that it is actually stable until after its freeze-out).<sup>3</sup> Since the NLSPs do not constitute CDM, we treat the quantity  $\Omega_{\text{NLSP}} h^2$  as a free parameter which will be determined experimentally at the LHC.

**Relic density and the LHC.** The total abundance of the LSPs is the sum of both thermal and non-thermal production contributions

$$\Omega_{\text{LSP}} h^2 = \Omega_{\text{LSP}}^{\text{TP}} h^2 + \Omega_{\text{LSP}}^{\text{NTP}} h^2. \quad (2.8)$$

Since it is natural to expect that the LSP makes up most of CDM in the Universe, we can re-write the above as

$$\Omega_{\text{LSP}}^{\text{TP}} h^2 (T_{\text{R}}, m_{\text{LSP}}, m_{\tilde{g}}, m_{\text{NLSP}}, \dots) + \frac{m_{\text{LSP}}}{m_{\text{NLSP}}} \Omega_{\text{NLSP}} h^2 = \Omega_{\text{LSP}} h^2 = \Omega_{\text{CDM}} h^2 \simeq 0.1. \quad (2.9)$$

This is our master formula. Once the neutralino NLSP is discovered and its mass is determined at the LHC with some precision, and so also  $\Omega_{\text{NLSP}} h^2 = \Omega_{\chi} h^2$ , then eq. (2.9) will provide a relation between  $T_{\text{R}}$  and  $m_{\text{LSP}}$ .

More specifically, in order to evaluate  $\Omega_{\chi} h^2$  at the LHC, the parameters determining the neutralino mass matrix will have to be evaluated through measurements at the LHC, as well as the masses of some other superpartners and Higgs boson(s) [3, 4]. For our purpose, also the mass of the gluino  $m_{\tilde{g}}$  will have to be known since it determines the efficiency of E-WIMP production in thermal scatterings. We assume the usual gaugino mass unification which, at the electroweak scale implies  $M_1 = 5/3 \tan^2 \theta_W M_2 = \alpha_1/\alpha_s m_{\tilde{g}}$  (or  $M_1 \simeq 0.5 M_2 \simeq m_{\tilde{g}}/6.5$ ), where  $M_1$  and  $M_2$  are the bino and wino mass parameters, respectively. (If the gluino mass is actually measured, we can use it in our expressions instead.) In this work we assume the lightest neutralino to be mostly a bino in which case  $m_{\chi} \simeq M_1 \simeq m_{\tilde{g}}/6.5$ .

Note that, if  $\Omega_{\text{NLSP}} h^2$  is determined to be larger than 0.1, the relic abundance of the LSP may easily agree with (1.1) by taking an appropriate mass ratio  $m_{\text{LSP}}/m_{\text{NLSP}}$  and

---

<sup>3</sup>Obviously, in our case  $\Omega_{\text{NLSP}} h^2$  is not the true cosmological relic abundance of the NLSPs. Instead it is simply given by  $\Omega_{\text{NLSP}} h^2 = m_{\text{NLSP}} Y_{\text{NLSP}} \frac{sh^2}{\rho_{\text{crit}}}$  where  $Y_{\text{NLSP}}$  is the NLSP yield at its freeze-out. Here, for convenience we will keep calling  $\Omega_{\text{NLSP}} h^2$  a “relic abundance”.



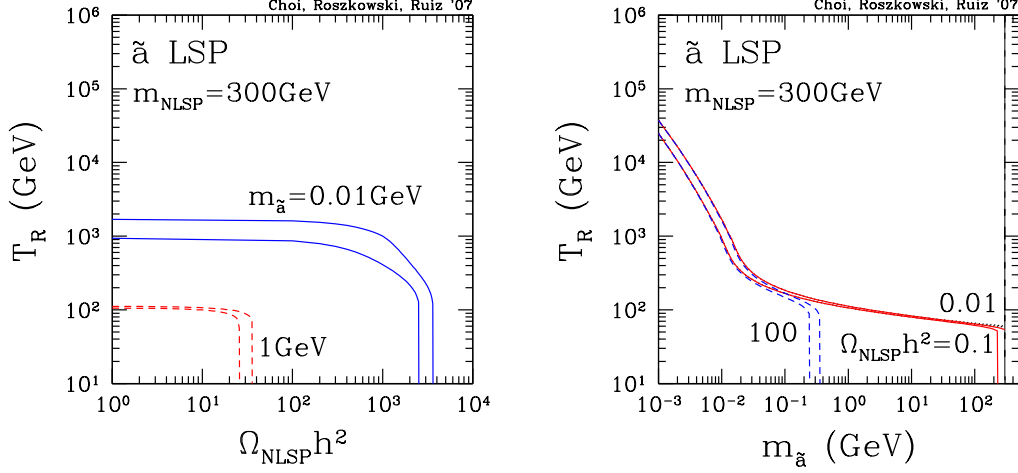


**Figure 2:** Left panel:  $T_R$  vs.  $\Omega_{\text{NLSP}} h^2$  for  $m_{\text{NLSP}} = 300 \text{ GeV}$  and for  $m_{\tilde{a}} = 0.01 \text{ GeV}$  (solid blue) and  $m_{\tilde{a}} = 1 \text{ GeV}$  (dashed red). The bands correspond to the upper and lower limits of dark matter density in (1.1). Right panel:  $T_R$  vs.  $m_{\tilde{a}}$  for  $\Omega_{\text{NLSP}} h^2 = 100$  (dashed blue), 0.1 (solid red) and 0.01 (dotted black). To the right of the solid vertical line the axino is no longer the LSP. In both panels we set  $f_a = 10^{11} \text{ GeV}$ .

small enough  $T_R$  in order to suppress TP. Should, on the other hand,  $\Omega_\chi h^2$  came out to be smaller than 0.1, a substantial contribution of LSP production in thermal processes at large enough  $T_R$  will be sufficient. Actually, TP may be dominant even if  $\Omega_\chi h^2$  is larger than, or for that matter is close to, 0.1, depending on the LSP and the neutralino NLSP mass ratio.

### 3. Axino dark matter

We first consider the axino as the LSP and the dominant component of DM in the Universe. As mentioned earlier, for definiteness we take the NLSP to be the lightest neutralino; the stau case will be considered below. It is reasonable to expect that LHC experiments will be able to probe neutralino (and stau) mass ranges up to some 400 GeV, depending on other SUSY parameters. Here we are not concerned with experimental uncertainties of LHC measurements but rather illustrate the principle of estimating  $T_R$  for a given DM candidate in terms of relation (2.9).

In the left panel of fig. 2 we show ranges of  $\Omega_{\text{NLSP}} h^2$  and  $T_R$ , such that  $\Omega_{\tilde{a}} h^2$  is in the range (1.1). We take a fixed neutralino NLSP mass  $m_{\text{NLSP}} = 300 \text{ GeV}$  and  $m_{\tilde{a}} = 0.01 \text{ GeV}$  (solid blue) and 1 GeV (dashed red). For each choice of the axino mass the two lines correspond to the upper and lower limits of dark matter density in (1.1). On the left side non-thermal production is subdominant while thermal production of axinos gives the main contribution to their relic density. In this case  $T_R$  corresponds to the value for which  $\Omega_{\tilde{a}}^{\text{TP}} h^2 \simeq \Omega_{\text{CDM}} h^2$ , and depends on the axino and NLSP masses since  $Y_{\tilde{a}}^{\text{TP}} \propto T_R / f_a^2$ . As  $\Omega_{\tilde{a}}^{\text{NTP}} h^2$  increases,  $\Omega_{\tilde{a}}^{\text{TP}} h^2$  must decrease (in order for the total abundance to remain close to

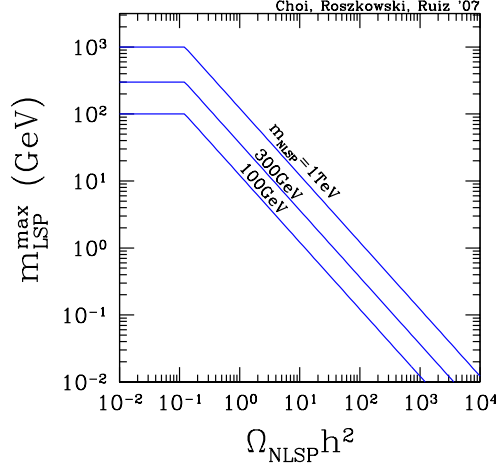


**Figure 3:** Maximum values of  $m_{\text{LSP}}$  as a function of  $\Omega_{\text{NLSP}} h^2$  for representative values of  $m_{\text{NLSP}}$ . Once both  $\Omega_{\text{NLSP}} h^2$  and  $m_{\text{NLSP}}$  are determined from experiment, the upper bound on  $m_{\text{LSP}}$  can be derived. The plot applies both to the axino and to the gravitino LSP.

0.1) and at some point becomes subdominant. This point is marked by an abrupt turnover of the contours from horizontal to vertical.

In the right panel of fig. 2 we plot  $m_{\tilde{a}}$  vs.  $T_{\text{R}}$  for the same NLSP mass and for  $\Omega_{\text{NLSP}} h^2 = 100$  (dashed blue), 0.1 (solid red) and 0.01 (dotted black). On the left side, where  $m_{\tilde{a}}$  is small, TP dominates,  $\Omega_{\tilde{a}}^{\text{TP}} h^2 \simeq \Omega_{\text{CDM}} h^2$ , hence we find

$$T_{\text{R}} \propto f_a^2 / m_{\tilde{a}}. \quad (3.1)$$

In this regime  $T_{\text{R}}$  is inversely proportional to the axino mass (for a given  $f_a$ , see below). (This dependence can be seen analytically by plugging eq. (2.5) into eq. (2.9) and taking the limit of negligible contribution from NTP.) The relation (3.1) allows one to derive an *upper bound* on  $T_{\text{R}}$  if we use the fact that axinos have to be heavy enough in order to constitute CDM. Assuming conservatively that  $m_{\tilde{a}} \gtrsim 100 \text{ keV}$  [15] we find  $T_{\text{R}}^{\text{max}} < 4.9 \times 10^5 \text{ GeV}$ .

At larger  $m_{\tilde{a}}$  the NTP contribution becomes dominant and the dependence on  $T_{\text{R}}$  is lost but one can still place a lower bound on  $T_{\text{R}}$ . Since in this regime the LSP mass becomes largest, this allows one to derive an *upper bound* on  $m_{\tilde{a}}$ . This is shown in fig. 3 as a function of  $\Omega_{\text{NLSP}} h^2$  for  $m_{\text{NLSP}} = 100, 300 \text{ GeV}$  and  $1 \text{ TeV}$ . Once both  $\Omega_{\text{NLSP}} h^2$  and  $m_{\text{NLSP}}$  are determined from experiment, the upper bound on  $m_{\text{LSP}}$  can be derived. Note that fig. 3 actually applies to both the axino and the gravitino LSP since it follows from eq. (2.7). On the other hand, the bound is interesting only if  $\Omega_{\text{NLSP}} h^2 \gg 0.1$ , otherwise it reduces to a trivial condition  $m_{\text{LSP}} < m_{\text{NLSP}}$ .

In fig. 4 we plot in the plane of varying  $m_{\text{NLSP}}$  and  $\Omega_{\text{NLSP}} h^2$  where contours of  $T_{\text{R}}$  for a fixed  $m_{\tilde{a}} = 0.01 \text{ GeV}$  (left panel) and  $1 \text{ GeV}$  (right panel). In the left panel, where  $m_{\tilde{a}}$  is tiny, for sufficiently large  $T_{\text{R}}$  thermal production dominates and the dependence on

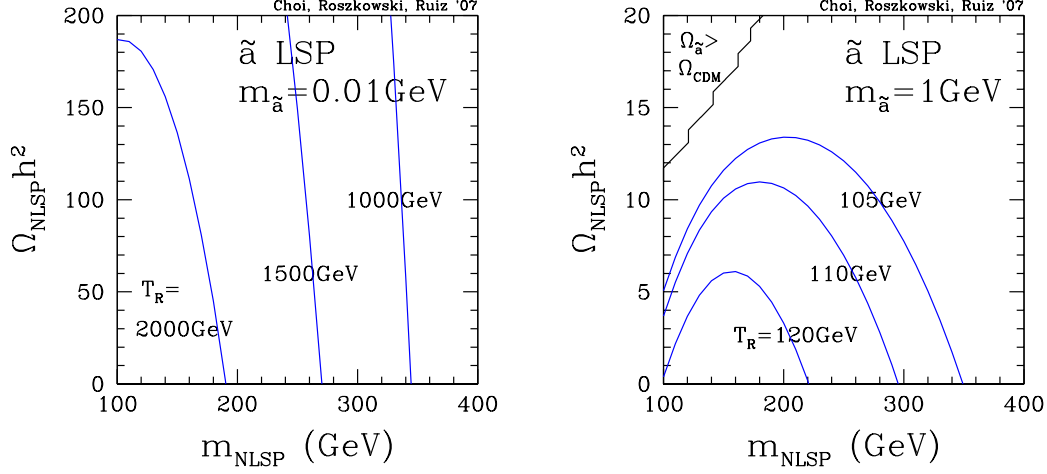


**Figure 4:** Contours of the reheating temperature in the plane of  $m_{\text{NLSP}}$  and  $\Omega_{\text{NLSP}} h^2$  such that  $\Omega_{\tilde{a}} h^2 = \Omega_{\text{CDM}} h^2 = 0.104$ . The axino mass is assumed to be 0.01 GeV (left panel) and 1 GeV (right).

$\Omega_{\text{NLSP}} h^2$  is very weak. Indeed, only at small  $m_{\tilde{a}}$  and large  $\Omega_{\text{NLSP}} h^2$  the NTP contribution  $\propto (m_{\tilde{a}}/m_{\text{NLSP}})\Omega_{\text{NLSP}} h^2$  starts playing some role.

On the other hand, in the right panel of fig. 4 the situation is somewhat more complex, with a characteristic turnover which depends on  $T_R$ . In order to explain it, in fig. 5 the TP and NTP contribution to the axino relic abundance are shown explicitly for one of the cases presented in fig. 4, along with the corresponding  $\Omega_{\text{NLSP}} h^2/100$ . As the neutralino mass  $m_\chi = m_{\text{NLSP}}$  increases, the gluino mass also increases (via the gaugino unification mass relation). So long as  $m_\chi \lesssim 130$  GeV, the gluino decay contribution to  $\Omega_{\tilde{a}}^{\text{TP}} h^2$  dominates over the one from squark decays (with squark masses fixed in here at 1 TeV) and from scatterings (compare the left panel of fig. 1), but it decreases from left to right. This is because it is proportional to  $m_{\tilde{g}}$  times an integral over the Boltzmann suppression factor  $\exp(-m_{\tilde{g}}/T)$ . On the other hand, the squark decay contribution, which scales as  $[m_{\tilde{g}}(1 - 0.05 \log(m_{\tilde{g}}/1 \text{ TeV}))]^2$ , increases [16]. Overall, as  $m_\chi$  increases, the TP part of  $\Omega_{\tilde{a}} h^2$  first decreases before increasing again. Thus the NTP part has to first increase and then decrease in order for the sum to remain constant at 0.104.

In the upper left-hand corner of the right panel of fig. 4, for a given ratio of  $m_{\tilde{a}}/m_{\text{NLSP}}$ ,  $\Omega_{\text{NLSP}} h^2$  becomes too large for  $\Omega_{\tilde{a}} h^2$  not to exceed 0.104, despite basically turning off the TP contribution (by reducing  $T_R$ ). As  $T_R$  increases, the Boltzmann suppression factor plays a smaller role and the TP part increases, thus making the NTP part decrease. This is why, for the same value of  $m_{\text{NLSP}}$ , the corresponding value of  $\Omega_{\text{NLSP}} h^2$  decreases with increasing  $T_R$ , in agreement with the right panel of fig. 4. Generally, for  $m_{\tilde{a}} = 1$  GeV the allowed values of  $T_R$  are much smaller than at smaller  $m_{\tilde{a}}$  (left panel).

In both figs. 2 and 4 we can see that a whole spectrum of values of  $\Omega_{\text{NLSP}} h^2$  coming out from LHC determinations can be consistent with the axino relic abundance satisfying  $\Omega_{\tilde{a}} h^2 \simeq 0.1$ . They can range from much smaller to those much larger than the “WMAP

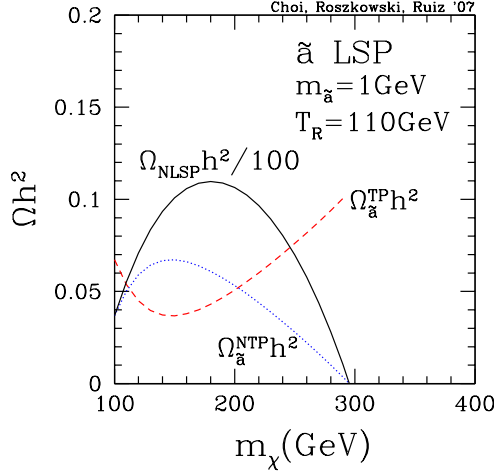


**Figure 5:** The TP (dashed red) and NTP (dotted blue) contributions to the axino relic abundance vs.  $m_{\text{NLSP}} = m_\chi$  for the case of  $m_{\tilde{a}} = 1 \text{ GeV}$  and  $T_R = 110 \text{ GeV}$  from fig. 8. The CDM relic abundance has been set at its central value of 0.104. Also shown is  $\Omega_{\text{NLSP}} h^2/100$  (solid black) for this case.

range” (1.1), depending on the mass of the LSP. Moreover,  $\Omega_{\text{NLSP}} h^2$  does not have to take largest values in the NTP-dominated case, as one would initially expect. On the other hand, when  $m_{\text{NLSP}}$  is much larger than  $m_{\text{LSP}}$ , NTP typically dominates, especially if  $\Omega_{\text{NLSP}} h^2$  is also large. On the other hand, if  $m_{\text{NLSP}}$  is not much larger than  $m_{\text{LSP}}$  and  $\Omega_{\text{NLSP}} h^2$  is also on the small side, then TP typically dominates. While this dependence is not rigorous, it may help one distinguishing between the TP and NTP-dominated regimes once  $m_{\text{NLSP}}$  and  $\Omega_{\text{NLSP}} h^2$  are experimentally determined.

Finally we comment on the dependence on  $f_a$ . Its value is limited to lie above some  $10^8 \text{ GeV}$  from cooling of red giants and below some  $10^{12} \text{ GeV}$  from inflation if it took place prior to the Peccei-Quinn transition. Otherwise larger values are allowed [30]. In our numerical examples we have set  $f_a = 10^{11} \text{ GeV}$ . Since only TP of axinos depends on  $f_a$  (as  $\Omega_{\tilde{a}}^{\text{TP}} h^2 \propto 1/f_a^2$ ) while NTP does not, in figs. 2 and 4 the regions dominated by TP will be affected accordingly. In other words,  $T_R \propto f_a^2/m_{\tilde{a}}$ , as stated above.

#### 4. Gravitino dark matter

The case of gravitino LSP, with its relic abundance  $\Omega_{\tilde{G}} h^2$  satisfying the range (1.1), can be analyzed in an completely analogous way, except for two important aspects.

The first has to do with Big Bang Nucleosynthesis (BBN). After the NLSPs freeze-out from thermal plasma and start decaying into the LSPs, energetic photons and hadronic jets are also produced. If this takes place during or after BBN, such particles may destroy successful predictions of standard BBN of light element abundances. In the axino LSP case, the NLSP decay occurs normally before BBN epoch begins [8, 15]. Thus the axino LSP is mostly free from BBN constraints. However, with gravitino couplings to ordinary matter being so much weaker, NLSP decays to gravitinos take place much later, varying

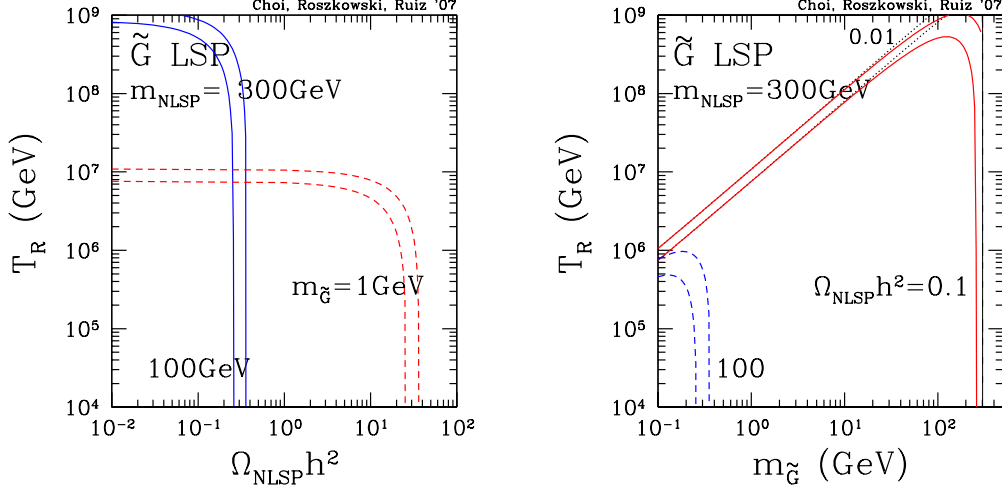


**Figure 6:** Left panel:  $T_R$  vs.  $\Omega_{\text{NLSP}} h^2$  for  $m_{\text{NLSP}} = 300 \text{ GeV}$  and for  $m_{\tilde{G}} = 0.01 \text{ GeV}$  (solid blue) and  $m_{\tilde{G}} = 1 \text{ GeV}$  (dashed red). The bands correspond to the upper and lower limits of dark matter density in (1.1). Right panel:  $T_R$  vs.  $m_{\tilde{G}}$  for  $\Omega_{\text{NLSP}} h^2 = 100$  (dashed blue), 0.1 (solid red) and 0.01 (dotted black). To the right of the solid vertical line the gravitino is no longer the LSP.

from 1 sec to  $10^{12}$  sec, depending on the masses of the two. Thus BBN usually provides severe constraints on the yield of the NLSP.

The neutralino NLSP is almost excluded with  $m_{\tilde{G}} \gtrsim 1 \text{ GeV}$  due to BBN [26, 28]. On the other hand, if the gravitino mass is less than  $\sim 1 \text{ GeV}$ , the lifetime of the neutralino becomes smaller than about 1 sec and the window of neutralino NLSP opens up again [28]. In our numerical examples below we will not impose the constraint from BBN but will indicate in which case it is satisfied or not.

The second important difference with the axino case was already discussed in sec. 2. While  $Y_a^{\text{TP}}$  is independent of the axino mass, in the gravitino case  $Y_{\tilde{G}}^{\text{TP}} \propto 1/m_{\tilde{G}}^2$ . Thus  $\Omega_a^{\text{TP}} h^2 \propto m_{\tilde{a}} T_R$  while  $\Omega_{\tilde{G}}^{\text{TP}} h^2 \propto T_R/m_{\tilde{G}}$ . In other words, if TP dominates,  $\Omega_{\tilde{G}}^{\text{TP}} h^2 \simeq 0.1$ , we find

$$T_R \propto m_{\tilde{G}}. \quad (4.1)$$

This is reflected in the right panel of fig. 6 where we show  $T_R$  vs.  $m_{\tilde{G}}$  for our nominal value of the NLSP mass of 300 GeV and for some fixed values of  $\Omega_{\text{NLSP}} h^2$ . So long as  $m_{\tilde{G}} \ll m_{\text{NLSP}}$  and  $\Omega_{\text{NLSP}} h^2$  is small enough, e.g.  $\Omega_{\text{NLSP}} h^2 = 0.1$  (denoted by a solid red curve), or less, the gravitino relic density is dominated by TP and  $T_R$  scales linearly with  $m_{\tilde{G}}$  so that  $\Omega_a^{\text{TP}} h^2 \simeq 0.1$ . On the other hand, when  $\Omega_{\text{NLSP}} h^2 = 100$  (dashed blue), NTP becomes rapidly dominant even with sub-GeV LSP mass. This can also be seen in the left panel of fig. 6 where we show  $T_R$  vs.  $\Omega_{\text{NLSP}} h^2$  for the same NLSP mass and for  $m_{\tilde{G}} = 0.01 \text{ GeV}$  (solid blue) and  $m_{\tilde{G}} = 1 \text{ GeV}$  (dashed red). For the smaller value of  $m_{\tilde{G}}$  the TP contribution remains dominant up to much larger allowed values of  $\Omega_{\text{NLSP}} h^2$  (horizontal part of the curves) before finally NTP takes over (vertical part). Note that, just like with the axino LSP case before, once we know  $m_{\text{NLSP}}$  and  $\Omega_{\text{NLSP}} h^2$ , we can place

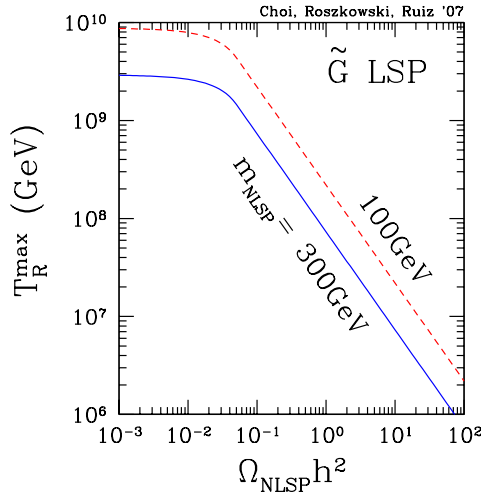


**Figure 7:** Maximum reheating temperature  $T_R^{\max}$  vs. NLSP relic density  $\Omega_{\text{NLSP}} h^2$  with gravitino DM for NLSP mass  $m_{\text{NLSP}} = 100 \text{ GeV}$  (dashed red) and  $300 \text{ GeV}$  (solid blue).

an *upper bound* on the mass of the gravitino assumed to be the dominant component of CDM in the Universe, see fig. 3.

The turnover between the TP and NTP dominance allows one to derive a conservative *upper bound*  $T_R^{\max}$  which, unlike for the axino CDM, even without knowing the gravitino mass. This can be seen from eqs. (2.6)–(2.8) from which an expression for  $T_R$  as a quadratic function of  $m_{\tilde{G}}$  can easily be found. Its maximum can then be expressed as

$$T_R^{\max} = \begin{cases} \frac{10^8 \text{ GeV}}{0.27} \left( \frac{1 \text{ TeV}}{m_{\tilde{g}}} \right)^2 \left( \frac{m_{\text{NLSP}}}{100 \text{ GeV}} \right) \frac{1}{4\Omega_{\text{NLSP}} h^2}, & \text{for } \Omega_{\text{NLSP}} h^2 > 0.05 \\ \frac{10^{10} \text{ GeV}}{0.27} \left( \frac{1 \text{ TeV}}{m_{\tilde{g}}} \right)^2 \left( \frac{m_{\text{NLSP}}}{100 \text{ GeV}} \right) (0.1 - \Omega_{\text{NLSP}} h^2), & \text{for } \Omega_{\text{NLSP}} h^2 < 0.05 \end{cases}, \quad (4.2)$$

where we have used  $\Omega_{\text{LSP}} h^2 = 0.1$ . This is plotted in fig. 7 for two representative choices of  $m_{\text{NLSP}} = 100, 300 \text{ GeV}$ , the former one being roughly the lowest value allowed by LEP.

In fig. 8 we present, in analogy with fig. 4, contours of  $T_R$  for a fixed  $m_{\tilde{G}} = 1 \text{ GeV}$  (left panel) and  $100 \text{ GeV}$  (right panel). In both, at sufficiently large  $\Omega_{\text{NLSP}} h^2$  we find a similar turnover of the contours as in the right panel of fig. 4 for the axino case. Again, in order to elucidate the situation, in fig. 9 the TP and NTP contributions to the gravitino relic abundance are explicitly shown for one of the cases presented in fig. 8, along with the corresponding  $\Omega_{\text{NLSP}} h^2 / 100$ , in analogy with fig. 5 for the axino case. The (initially subdominant) TP part increases with increasing  $m_{\tilde{g}}$  (which grows with  $m_{\chi}$ ), thus the NTP part has to decrease in order for the sum to remain constant at 0.104. In the upper left-hand corner of both panels of fig. 8, for a given ratio of  $m_{\tilde{G}}/m_{\text{NLSP}}$ ,  $\Omega_{\text{NLSP}} h^2$  becomes too large and  $\Omega_{\tilde{G}} h^2$  exceeds 0.104, despite basically turning off the TP contribution (by reducing  $T_R$ ).

In the gravitino LSP case it is easy to derive a simple expression for the value of the NLSP mass at which the turnover in  $\Omega_{\text{NLSP}} h^2$  in fig. 8 takes place. By taking the NLSP to

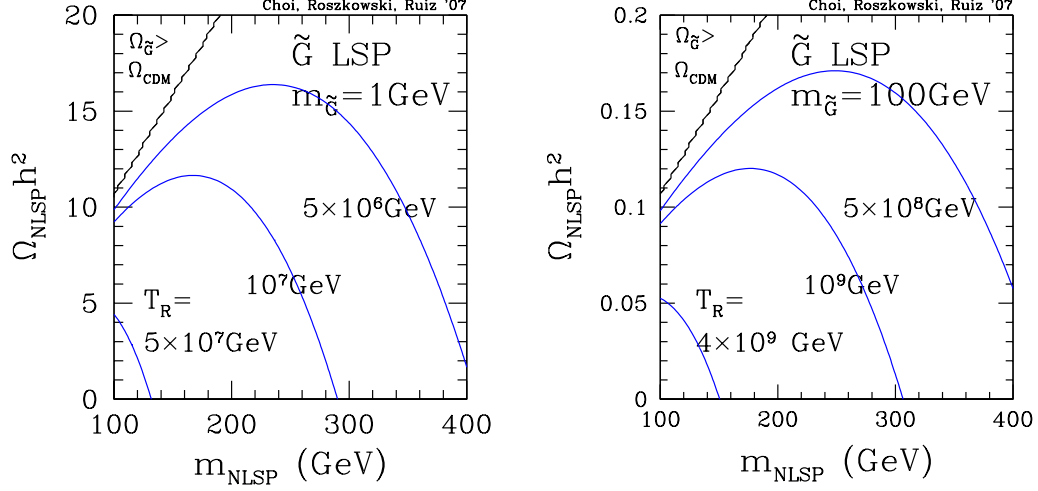


**Figure 8:** Contours of the reheating temperature in the plane of  $m_{\text{NLSP}}$  and  $\Omega_{\text{NLSP}} h^2$  such that  $\Omega_{\tilde{G}} h^2 = \Omega_{\text{CDM}} h^2 = 0.104$ . The gravitino mass is assumed to be 1 GeV (left panel) and 100 GeV (right panel).

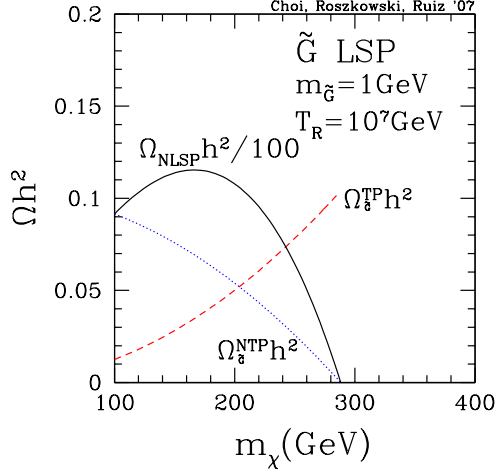


**Figure 9:** The TP (dashed red) and NTP (dotted blue) contributions to the gravitino relic abundance vs.  $m_{\text{NLSP}} = m_\chi$  for the case of  $m_{\tilde{G}} = 1$  GeV and  $T_R = 10^7$  GeV from fig. 8. The CDM relic abundance has been set at its central value of 0.104. Also shown is  $\Omega_{\text{NLSP}} h^2 / 100$  (solid black) for this case.

be the bino (as we do in our numerical examples), plugging the expression for  $\Omega_{\tilde{G}}^{\text{TP}} h^2$  from eq. (2.6) into eq. (2.9) and making a simplifying assumption  $m_{\tilde{g}}(\mu) \simeq m_{\tilde{g}} \simeq 6.5 m_\chi$  one obtains an expression for  $\Omega_\chi h^2$  as a cubic function of  $m_\chi$ . By putting its first derivative to zero one arrives at

$$m_\chi \simeq 54 \left( \frac{10^{10} \text{ GeV}}{T_R} \right)^{1/2} \left( \frac{m_{\tilde{G}}}{10^2 \text{ GeV}} \right)^{1/2} \text{ GeV}, \quad (4.3)$$

which adequately reproduces the positions of the peaks in fig. 8.

The case of  $m_{\tilde{G}} = 1 \text{ GeV}$  is on the borderline of being consistent with BBN, while the mass of  $100 \text{ GeV}$  is not (if the NLSP is the neutralino). On the other hand, both cases can be allowed for some choices of MSSM parameters if the NLSP is the stau, see below. Note that in the gravitino case resulting values of  $T_R$  are typically significantly larger than for axinos. On the other hand, for sufficiently small  $m_{\tilde{G}} \lesssim 1 \text{ GeV}$  (roughly consistent with BBN constraints for NLSP neutralino) we find  $T_R \sim 10^{6-7} \text{ GeV}$ , while for MeV-mass axinos  $T_R \sim 10^{4-5} \text{ GeV}$  (compare the right panel of fig. 2), which are of similar order.

## 5. Stau NLSP

Finally, we discuss the case of the lighter stau as the NLSP. Its couplings are of a sufficiently similar size to those of the neutralino that, for the same mass, its freeze-out temperature and yield are basically the same, hence is also its NTP contribution to either axino or gravitino relic abundance. For this reason, our numerical results presented in figs. 2–8 for the neutralino NLSP case apply directly to the stau NLSP case.<sup>4</sup>

What is different is the impact of BBN constraints. Like with the neutralino, stau decays result in both electromagnetic and hadronic showers. Axino production from NLSP decays mostly takes place before the period of BBN, thus this case remains basically unconstrained. On the hand, the gravitino LSP case is again strongly constrained. Detailed analyses have shown that BBN constraints are somewhat weaker with stau NLSP than for the neutralinos [26, 27, 28]. As a result, the LSP gravitino mass in the range of tens, or even hundreds, of GeV, can remain allowed and consistent with  $\Omega_{\tilde{G}} h^2$  in the “WMAP range”. Stau NLSP is also disallowed if its lifetime is longer than about  $10^3 \text{ sec}$ , as otherwise it would form metastable bound states with nuclei which would affect BBN abundances of light elements, as recently pointed out in [31], see also [32, 33]. The stau lifetime is dominated by two-body decay to tau and gravitino which, neglecting tau mass, is given by [26]

$$\tau(\tilde{\tau} \rightarrow \tau + \tilde{G}) = 6.1 \times 10^3 \text{ sec} \left( \frac{1 \text{ TeV}}{m_{\tilde{\tau}}} \right)^5 \left( \frac{m_{\tilde{G}}}{100 \text{ GeV}} \right)^2 \left( 1 - \frac{m_{\tilde{G}}^2}{m_{\tilde{\tau}}^2} \right)^{-4}. \quad (5.1)$$

In our numerical example in the right panel of fig. 6, with  $m_{\tilde{\tau}} = 300 \text{ GeV}$ , where we have also taken  $m_{\chi} = 477 \text{ GeV}$ , the condition  $\tau_{\tilde{\tau}} > 10^3 \text{ sec}$  implies  $m_{\tilde{G}} \lesssim 2 \text{ GeV}$  and  $T_R \lesssim 9 \times 10^6 \text{ GeV}$ . Increasing  $m_{\tilde{\tau}}$  to  $1 \text{ TeV}$  and  $m_{\chi}$  to  $1.5 \text{ TeV}$  leads to  $m_{\tilde{G}} \lesssim 40 \text{ GeV}$  and  $T_R \lesssim 4 \times 10^8 \text{ GeV}$ .

The main point is that, with the neutralino NLSP, BBN constraints basically exclude gravitino CDM with the mass larger than about  $1 \text{ GeV}$ , while in the stau NLSP case much larger values can be allowed.

## 6. Summary

If the axino or the gravitino E-WIMP is the lightest superpartner and the dominant component of CDM in the Universe, then, under favorable conditions, it will be possible to

---

<sup>4</sup>One caveat is that the gluino mass, which is important in TP, is not directly related anymore to the stau mass.



determine the reheating temperature after inflation from LHC measurements. Basically, one will need to measure the neutralino mass and other parameters determining its “relic abundance” - a non-trivial and highly exciting possibility in itself. The quantity may be found to be different from the “WMAP range” (1.1), thus suggesting a non-standard CDM candidate. Additionally, one will need to know the mass of the gluino, either through a direct measurement, or via the gaugino unification mass relation, since it plays an important role in E-WIMP production at high  $T_R$ . The neutralino is likely to be sufficiently long-lived to appear stable in LHC detectors, but in the early Universe it would have decayed into the axino or the gravitino LSP. Since each of them is extremely weakly interacting, it would be hopeless to look for them in usual WIMP dark matter searches.

In the axino LSP case, if thermal production dominates, a consistency of its relic abundance with the “WMAP range” (1.1) implies  $T_R \propto f_a^2/m_{\tilde{a}}$ . If non-thermal production is dominant instead, then, for a known value of  $m_\chi$ , the value of  $\Omega_\chi h^2$  will imply an upper bound on  $m_{\tilde{a}}/f_a^2$ , which in turn will imply a lower bound on  $T_R$ .

For the gravitino LSP, in the thermal production dominated case the analogous dependence is  $T_R \propto m_{\tilde{G}}$ . If non-thermal production dominates then the value of  $\Omega_\chi h^2$  will imply an upper bound on  $m_{\tilde{G}}$ . For both axino and gravitino one can express this as

$$m_{\text{LSP}}^{\text{max}} = \min\{m_{\text{NLSP}}, \frac{\Omega_{\text{CDM}} h^2}{\Omega_{\text{NLSP}} h^2} m_{\text{NLSP}}\}, \quad (6.1)$$

which is independent of  $T_R$ .

For both relics, one can also derive an upper bound on  $T_R$ , although in the axino case has to further assume that it is cold DM. On the other hand, for both axino and gravitino, it will be difficult to distinguish between the TP and NTP regimes but some information may be helpful. Typically, when  $m_\chi$  is large and  $\Omega_{\text{NLSP}} h^2$  is also large then NTP is dominant, while if  $\Omega_{\text{NLSP}} h^2$  is small then TP typically dominates.

Similar conclusions as for the neutralino (for both E-WIMPs) apply if the NLSP is the stau, instead. Additionally, the very discovery of a charged, massive and (seemingly) stable state at the LHC will immediately imply that dark matter in the Universe is not made up of the usual neutralino.

With so many similarities between both E-WIMPs, a natural question arises whether it would be possible to distinguish them in a collider experiment. Unfortunately, with neutralino NLSP this is unlikely to be possible. On the other hand, with the stau NLSP being electrically charged, enough of them could possibly be accumulated. By comparing their 3-body decays, it may be possible to only tell whether Nature has selected the axino or the gravitino as the lightest superpartner, but to actually also determine their mass with some reasonable precision [34, 29]. Needless to say, this would allow one to determine also the reheating temperature.

In this work, we focused on demonstrating the principle of determining  $T_R$  at the LHC, and did not concern ourselves with uncertainties of experimental measurements. These are likely to be substantial at the LHC, the case we have mostly focused on here, unless one considers specific models [5]. A more detailed study will be required to assess their impact. An analogous study can be performed in the context of the planned Linear

Collider. We also implicitly assumed that only one relic dominates the CDM component of the Universe, which in principle does not have to be the case. For example, the axion and the axino could co-exist and contribute comparable fractions to the CDM relic density. (Note that this could be the case also in the “standard” case of the stable neutralino.) This would introduce an additional uncertainty and would lead to replacing the derived values of  $T_R$  with an upper bound on the quantity.

### Acknowledgements

This work is supported by an STFC grant. K.-Y.C. has been partially supported by a PPARC grant, by the Ministerio de Educacion y Ciencia of Spain under Proyecto Nacional FPA2006-05423 and by the Comunidad de Madrid under Proyecto HEPHACOS, Ayudas de I+D S-0505/ESP-0346. L.R is partially supported by the EC 6th Framework Programmes MRTN-CT-2004-503369 and MRTN-CT-2006-035505. R.RdA is supported by the program “Juan de la Cierva” of the Ministerio de Educación y Ciencia of Spain. The author(s) would like to thank CERN for hospitality and support and the European Network of Theoretical Astroparticle Physics ENTApP ILIAS/N6 under contract number RII3-CT-2004-506222 for support. This project benefited from the CERN-ENTApP joint visitor’s programme on dark matter, 5-9 March 2007 and the CERN Theory Institute “LHC-Cosmology Interplay”, 25 June - 10 Aug 2007.

### References

- [1] See, e.g., G. Jungman, M. Kamionkowski and K. Griest, *Supersymmetric dark matter*, *Phys. Rept.* **267** (1996) 195;  
C. Muñoz, *Dark Matter Detection in the Light of Recent Experimental Results*, *Int. J. Mod. Phys. A* **19** (2004) 3093 [hep-ph/0309346];  
G. Bertone, D. Hooper and J. Silk, *Particle Dark Matter: Evidence, Candidates and Constraints*, *Phys. Rept.* **405** (2005) 279 [hep-ph/0404175].
- [2] D. N. Spergel, *et al.* [WMAP Collaboration], *Wilkinson Microwave Anisotropy Probe (WMAP) three year results: Implications for cosmology*, *Astrophys. J. Supp.* **170** (2007) 377 [astro-ph/0603449].
- [3] G. Polesello and D. R. Tovey, *Constraining SUSY dark matter with the ATLAS detector at the LHC*, *J. High Energy Phys.* **0405** (2004) 071 [hep-ph/0403047].  
See also B. C. Allanach, G. Belanger, F. Boudjema, A. Pukhov, *Requirements on collider data to match the precision of WMAP on supersymmetric dark matter*, *J. High Energy Phys.* **0412** (2004) 020 [hep-ph/0410091v2] and  
E. A. Baltz, M. Battaglia, M. E. Peskin, T. Wizansky, *Determination of Dark Matter Properties at High-Energy Colliders*, *Phys. Rev. D* **74** (2006) 103521 [hep-ph/0602187v4].
- [4] M. M. Nojiri, G. Polesello and D. R. Tovey, *Constraining dark matter in the MSSM at the LHC*, *J. High Energy Phys.* **0603** (2006) 063 [hep-ph/0512204].
- [5] See, e.g., J. L. Bourjaily and G. L. Kane, *What is the Cosmological Significance of a Discovery of Wimps at Colliders or in Direct Experiments?*, hep-ph/0501262.
- [6] M. Battaglia, *Study of Dark Matter inspired cMSSM scenarios at a TeV-class Linear Collider*, hep-ph/0410123v1;

- A. Birkedal *et al.*, *Testing cosmology at the ILC*, hep-ph/0507214;  
T. Moroi, Y. Shimizu, A. Yotsuyanagi, *Reconstructing Dark Matter Density with  $e^+e^-$  Linear Collider in Focus-Point Supersymmetry*, *Phys. Lett. B* **625** (2005) 79 [hep-ph/0505252v2].
- [7] J. Angle, *et al.*, *First Results from the XENON10 Dark Matter Experiment at the Gran Sasso National Laboratory*, *Phys. Rev. Lett.* **100** (2008) 021303 [arXiv:0706.0039v2];  
The CDMS Collaboration, *Limits on spin-independent WIMP-nucleon interactions from the two-tower run of the Cryogenic Dark Matter Search*, *Phys. Rev. Lett.* **96** (2006) 011302 [astro-ph/0509259];  
V. Sanglard *et al.* [EDELWEISS Collaboration], *Final results of the EDELWEISS-I dark matter search with cryogenic heat-and-ionization Ge detectors*, *Phys. Rev. D* **71** (2005) 122002 [astro-ph/0503265];  
G. J. Alner *et al.* [UK Dark Matter Collaboration], *First limits on nuclear recoil events from the ZEPLIN-I galactic dark matter detector*, *Astropart. Phys.* **23** (2005) 444.
- [8] L. Covi, J. E. Kim and L. Roszkowski, *Axinos as cold dark matter*, *Phys. Rev. Lett.* **82** (1999) 4180 [hep-ph/9905212].
- [9] P. Salati, *Quintessence and the relic density of neutralinos*, *Phys. Lett. B* **571** (2003) 121 [astro-ph/0207396];  
F. Rosati, *Quintessential enhancement of dark matter abundance*, *Phys. Lett. B* **570** (2003) 5 [hep-ph/0302159];  
S. Profumo and P. Ullio, *SUSY dark matter and quintessence*, *J. Cosmol. Astrop. Phys.* **0311** (2003) 006 [hep-ph/0309220];  
R. Catena, N. Fornengo, A. Masiero, M. Pietroni and F. Rosati, *Dark matter relic abundance and scalar-tensor dark energy*, *Phys. Rev. D* **70** (2004) 063519 [astro-ph/0403614];  
C. Pallis, *Quintessential kination and cold dark matter abundance*, *J. Cosmol. Astrop. Phys.* **0510** (2005) 015 [hep-ph/0503080] and *Kination dominated reheating and cold dark matter abundance*, *Nucl. Phys. B* **751** (2006) 129 [hep-ph/0510234];  
R. Rosenfeld, *Relic abundance of mass-varying cold dark matter particles*, *Phys. Lett. B* **624** (2005) 158 [astro-ph/0504121];  
G. Barenboim and J. D. Lykken, *Colliders as a simultaneous probe of supersymmetric dark matter and Terascale cosmology*, *J. High Energy Phys.* **0612** (2006) 005 [hep-ph/0608265];  
D. J. H. Chung, L. L. Everett and K. T. Matchev, *Inflationary Cosmology Connecting Dark Energy and Dark Matter*, *Phys. Rev. D* **76** (2007) 103530 [arXiv:0704.3285 [hep-ph]].
- [10] G. F. Giudice, E. W. Kolb and A. Riotto, *Largest temperature of the radiation era and its cosmological implications*, *Phys. Rev. D* **64** (2001) 023508 [hep-ph/0005123].
- [11] C. Pallis, *Massive Particle Decay and Cold Dark Matter Abundance*, *Astropart. Phys.* **21** (2004) 689 [hep-ph/0402033];  
G. B. Gelmini and P. Gondolo, *Neutralino with the Right Cold Dark Matter Abundance in (Almost) Any Supersymmetric Model*, *Phys. Rev. D* **74** (2006) 023510 [hep-ph/0602230];  
G. B. Gelmini, P. Gondolo, A. Soldatenko and C. E. Yaguna, *The effect of a late decaying scalar on the neutralino relic density*, *Phys. Rev. D* **74** (2006) 083514 [hep-ph/0605016].
- [12] K. Y. Choi and L. Roszkowski, *E-WIMPs*, *AIP Conf. Proc.* **805** (2006) 30 [hep-ph/0511003].
- [13] E.J. Chun, J.E. Kim and H.P. Nilles, *Phys. Lett. B* **287** (1992) 123;  
E.J. Chun and A. Lukas, *Phys. Lett. B* **357** (1995) 43.
- [14] J. E. Kim, *Weak Interaction Singlet And Strong CP Invariance*, *Phys. Rev. Lett.* **43** (1979) 103;

- M.A. Shifman, V.I. Vainstein and V.I. Zakharov, *Can Confinement Ensure Natural CP Invariance Of Strong Interactions?* *Nucl. Phys. B* **166** (1980) 493.
- [15] L. Covi, H. B. Kim, J. E. Kim and L. Roszkowski, *Axinos as dark matter*, *J. High Energy Phys.* **0105** (2001) 033 [hep-ph/0101009].
  - [16] L. Covi, L. Roszkowski and M. Small, *Effects of squark processes on the axino CDM abundance*, *J. High Energy Phys.* **0207** (2002) 023 [hep-ph/0206119].
  - [17] L. Covi, L. Roszkowski, R. Ruiz de Austri and M. Small, *Axino dark matter and the CMSSM*, *J. High Energy Phys.* **0406** (2004) 003 [hep-ph/0402240].
  - [18] A. Brandenburg and F. D. Steffen, *Axino dark matter from thermal production*, *J. Cosmol. Astrop. Phys.* **0408** (2004) 008 [hep-ph/0405158].
  - [19] V. S. Rychkov and A. Strumia, *Thermal production of gravitinos*, *Phys. Rev. D* **75** (2007) 075011 [hep-ph/0701104].
  - [20] K. Rajagopal, M.S. Turner and F. Wilczek, *Cosmological implications of axinos*, *Nucl. Phys. B* **358** (1991) 447.
  - [21] Early papers on the gravitino as a cosmological relic include: A.D. Dolgov and Ya.B. Zel'dovich, *Cosmology And Elementary Particles*, *Rev. Mod. Phys.* **53** (1981) 1; H. Pagels and J.R. Primack, *Supersymmetry, Cosmology And New Tev Physics*, *Phys. Rev. Lett.* **48** (1982) 223; S. Weinberg, *Cosmological Constraints On The Scale Of Supersymmetry Breaking*, *Phys. Rev. Lett.* **48** (1982) 1303; M.Y. Khlopov and A. Linde, *Is It Easy To Save The Gravitino?*, *Phys. Lett. B* **138** (1984) 265; J.R. Ellis, D.V. Nanopoulos and S. Sarkar, *The Cosmology Of Decaying Gravitinos*, *Nucl. Phys. B* **259** (1985) 175; D.V. Nanopoulos, K.A. Olive and M. Srednicki, *After Primordial Inflation*, *Phys. Lett. B* **127** (1983) 30; R. Juszkiewicz, J. Silk and A. Stebbins, *Constraints on cosmologically regenerated gravitinos*, *Phys. Lett. B* **158** (1985) 463.
  - [22] J.R. Ellis, J.E. Kim and D.V. Nanopoulos, *Cosmological Gravitino Regeneration And Decay*, *Phys. Lett. B* **145** (1984) 181.
  - [23] T. Moroi, H. Murayama and M. Yamaguchi, *Cosmological constraints on the light stable gravitino*, *Phys. Lett. B* **303** (1993) 289.
  - [24] M. Bolz, W. Buchmüller and Plümacher, *Baryon asymmetry and dark matter*, *Phys. Lett. B* **443** (1998) 209 [hep-ph/9809381].
  - [25] M. Bolz, A. Brandenburg and W. Buchmüller, *Thermal Production of Gravitinos*, *Nucl. Phys. B* **606** (2001) 518 [hep-ph/0012052].
  - [26] J.L. Feng, A. Rajaraman and F. Takayama, *Superweakly-interacting massive particles*, *Phys. Rev. Lett.* **91** (2003) 011302 [hep-ph/0302215]; J.L. Feng, A. Rajaraman and F. Takayama, *SuperWIMP dark matter signals from the early universe*, *Phys. Rev. D* **68** (2003) 063504 [hep-ph/0306024]; J. L. Feng, S. f. Su and F. Takayama, *SuperWIMP gravitino dark matter from slepton and sneutrino decays*, *Phys. Rev. D* **70** (2004) 063514 [hep-ph/0404198] and *Supergravity with a gravitino LSP*, prd702004075019 [hep-ph/0404231].

- [27] L. Roszkowski, R. Ruiz de Austri and K. Y. Choi, *Gravitino dark matter in the CMSSM and implications for leptogenesis and the LHC*, *J. High Energy Phys.* **0508** (2005) 080 [hep-ph/0408227].
- [28] D. G. Cerdeno, K. Y. Choi, K. Jedamzik, L. Roszkowski and R. Ruiz de Austri, *Gravitino dark matter in the CMSSM with improved constraints from BBN*, *J. Cosmol. Astrop. Phys.* **0606** (2006) 005 [hep-ph/0509275].
- [29] A. Brandenburg, L. Covi, K. Hamaguchi, L. Roszkowski and F. D. Steffen, *Signatures of axinos and gravitinos at colliders*, *Phys. Lett. B* **617** (2005) 99 [hep-ph/0501287].
- [30] F. Wilczek, *Anticipating a New Golden Age*, arXiv:0708.4236 [hep-ph].
- [31] M. Pospelov, *Particle physics catalysis of thermal big bang nucleosynthesis*, *Phys. Rev. Lett.* **98** (2007) 231301 [hep-ph/0605215].
- [32] C. Bird, K. Koopmans and M. Pospelov, *Primordial Lithium Abundance in Catalyzed Big Bang Nucleosynthesis*, hep-ph/0703096.
- [33] M. Kaplinghat and A. Rajaraman, *Big bang nucleosynthesis with bound states of long-lived charged particles*, *Phys. Rev. D* **74** (2006) 103004 [astro-ph/0606209].
- [34] W. Buchmuller, K. Hamaguchi, M. Ratz and T. Yanagida, “*Supergravity at Colliders*”, *Phys. Lett. B* **588** (2004) 90 [hep-ph/0402179v2].